NeuroImage 191 (2019) 36–48

Contents lists available at ScienceDirect

NeuroImage

journal homepage: www.elsevier.com/locate/neuroimage

The emergence of long-range language network structural covariance and language abilities

Ting Qi [a,*], Gesa Schaadt [a,b], Riccardo Cafiero [a], Jens Brauer [a], Michael A. Skeide [a], Angela D. Friederici [a]

[a] Department of Neuropsychology, Max Planck Institute for Human Cognitive and Brain Sciences, Leipzig, Germany
[b] Department of Neurology, Max Planck Institute for Human Cognitive and Brain Sciences, Leipzig and Clinic of Cognitive Neurology, Medical Faculty, University Leipzig, Germany

ARTICLE INFO

Keywords:
Language development
Syntax
Structural covariance
Cortical thickness
Five-year-olds
Diffusion-weighted imaging

ABSTRACT

Language skills increase as the brain matures. Language processing, especially the comprehension of syntactically complex sentences, is supported by a brain network involving functional interactions between left inferior frontal and left temporal regions in the adult brain, with reduced functional interactions in children. Here, we examined the gray matter covariance of the cortical thickness network relevant for syntactic processing in relation to language abilities in preschool children (i.e., 5-year-olds) and analyzed the developmental changes of the cortical thickness covariance cross-sectionally by comparing preschool children, school age children, and adults. Further, to demonstrate the agreement of cortical thickness covariance and white matter connectivity, tractography analyses were performed. Covariance of language-relevant seeds in preschoolers was strongest in contralateral homologous regions. A more adult-like, significant cortical thickness covariance between left frontal and left temporal regions, however, was observed in preschoolers with advanced syntactic language abilities. By comparing the three age groups, we could show that the cortical thickness covariance pattern from the language-associated seeds develops progressively from restricted in preschoolers to widely-distributed brain regions in adults. In addition, our results suggest that the cortical thickness covariance difference of the left inferior frontal gyrus to superior temporal gyrus/sulcus between preschoolers and adults is accompanied by distinctions in the white matter tracts linking these two areas, with more mature white matter in the arcuate fasciculus in adults compared to preschoolers. These findings provide anatomical evidence for developmental changes in language both from the perspective of gray matter structure co-variation within the language network and white matter maturity as the anatomical substrate for the structural covariance.

1. Introduction

The brain's structure undergoes remarkable changes during human development and scales up with individual differences in behavior and cognitive functions, such as intelligence and memory (Giedd et al., 1999; Kanai and Rees, 2011; Shaw et al., 2008; Sowell, 2004; Sowell et al., 2004). The interest in structural connectivity of the cerebral cortex has recently been emphasized in human brain research, stressing that cognitive functions are supported by connections between distributed, rather than isolated cortical regions (Fedorenko and Thompson-Schill, 2014). One approach for aspects of cortical networks is structural covariance, describing the phenomenon that gray matter properties of one brain region may co-vary with those of other broadly distributed cortical regions (Alexander-Bloch et al., 2013a). It has been assumed that structural covariance is related to axonal connectivity and that it underlies functional connectivity between regions as a result of mutually trophic influences (Ferrer et al., 1995), shared experience-related plasticity (Draganski et al., 2004; Mechelli, 2005; Montembeault et al., 2012), or a combination of these factors (Seeley et al., 2009). Like for the brain's gray and white matter, structural covariance has also been observed to change with age, as well as to interact with behavioral and cognitive functions and its disorders (Alexander-Bloch et al., 2013a; Bernhardt et al., 2014b; Montembeault et al., 2016; Qi et al., 2016; Seeley et al., 2009). For instance, for children up to the age of 2 years,

* Corresponding author. Department of Neuropsychology, Max Planck Institute for Human Cognitive and Brain Sciences, Stephanstrasse 1a, Leipzig, 04103, Germany.
E-mail address: tingqi@cbs.mpg.de (T. Qi).

https://doi.org/10.1016/j.neuroimage.2019.02.014
Received 24 September 2018; Received in revised form 28 January 2019; Accepted 5 February 2019
Available online 7 February 2019
1053-8119/

structural covariance has been observed to be restricted by showing mostly correlations with the surrounding regions of the seed for both higher-order (e.g., default-mode, dorsal attention, speech, semantic, and executive control networks) and lower-order networks (e.g., primary visual and sensorimotor networks) (Geng et al., 2016). Between the ages 5 and 18 years, diverging developmental trajectories for lower- and higher-order networks were shown. The lower-order networks demonstrate well-established structural covariance already in early childhood, peaking in early adolescence, before pruning induces further reorganization towards adulthood. In contrast, structural covariance of higher-order networks is not yet fully developed in early childhood, which is mainly characterized by co-variation between contralateral homologous regions. The structural covariance of higher-order networks then develops progressively to more widely distributed regions across the teenage years (Zielinski et al., 2010). A similar developmental pattern has been demonstrated for intrinsic functional connectivity with increased short-range and sparse long-range functional connectivity in children, but a coherent long-range architecture in young adults across a range of cognitive networks (i.e., control and default mode networks) (Fair et al., 2009, 2007; Kelly et al., 2009; Supekar et al., 2009). Thus, developmental findings for both functional and structural covariance networks suggest that our brain develops by pruning short-range connections and strengthening long-range connections (Hagmann et al., 2010).

Structural covariance has also been suggested to be associated with behavioral and cognitive abilities, such as working memory, intellectual abilities, and vocabulary abilities, in developing children and adults (Lee et al., 2014; Lerch et al., 2006; Oh et al., 2011). For instance, children with higher intelligence were shown to have stronger thickness covariance between the left inferior frontal region and other frontal and parietal regions (Lerch et al., 2006). Furthermore, typically developing children with higher vocabulary skills were shown to have greater thickness covariance in language-related regions, including left inferior parietal, inferior temporal, and middle frontal regions (Lee et al., 2014). Similar to other higher cognitive functions, language processes require a highly specialized network within which the distributed areas subserving the relevant processes are integrated. In contrast to vocabulary skills, however, little is known about the cortico-cortical structural covariance network of cortical thickness underlying syntax - a crucial component of the language processing system.

In previous studies using a variety of different tasks, a left temporo-frontal network (perisylvian cortex) has been identified as language-specific (Fedorenko et al., 2011; Lohmann et al., 2010). In particular, the left inferior frontal and posterior superior temporal lobe have been suggested to be involved in the comprehension of syntactically complex sentences in adults (Friederici, 2011, 2009; Grewe et al., 2007; Kinno et al., 2008; Makuuchi et al., 2009; Meltzer et al., 2010; Santi and Grodzinsky, 2010). From the perspective of development, the processing of syntactically complex sentences develops slowly and gradually in children (Skeide and Friederici, 2016). Three-year-old children are able to detect grammatical case-marking cues, but are not able to use this information for sentence comprehension until the age of six years (Schipke et al., 2012). The reason for this slow and gradual development of the processing of syntactically complex sentences can be found in studies examining the functional and structural developmental trajectories of the language-specific brain network. From the functional perspective, for example, preschoolers show reduced activation in the left inferior frontal and superior temporal regions during sentence processing compared to adults (Brauer and Friederici, 2007; Friederici et al., 2011; Wu et al., 2016). Interestingly, this long-range functional connectivity of language relevant brain regions was positively correlated with the preschoolers' competences to process syntactically complex sentences, suggesting individual abilities to be interrelated with the brain's functional development (Xiao et al., 2016). Further, although children start to show functional selectivity in the left posterior superior temporal gyrus (pSTG) between the ages of 9–10 years, they still do not show any adult-like functional selectivity in the left BA44 - a core region for syntactic processes - during syntactic processing (Skeide et al., 2016). Moreover, from the anatomical perspective, a positive correlation was found between sentence comprehension abilities and the gray matter volume of the left inferior frontal gyrus (IFG), inferior temporal gyrus (ITG), and the left parieto-temporal regions in children between the ages of 5–8 years (Fengler et al., 2015). In addition, the fractional anisotropy (FA) of the arcuate fasciculus, referred to as the dorsal language pathway connecting the left IFG and the pSTG (Frey et al., 2008; Wilson et al., 2011), was positively correlated with the sentence comprehension abilities in children between the ages of 3–10 years (Skeide et al., 2016). The dorsal language pathway, which has been suggested to be crucial for syntactic processing, does not fully mature until late childhood (Brauer et al., 2011; Perani et al., 2011). Furthermore, concerning cortical thickness covariance in adolescents, it was found that the cortical thickness of BA44 was co-varied with the thickness in the temporal regions, and this covariance was further suggested to change with age (Lerch et al., 2006). Together, functional and white matter structural connectivity of language-relevant brain regions has been shown to develop across childhood and to be influenced by individual language abilities. However, the development of the cortical thickness covariance of language-relevant brain regions and its relation to syntactic language abilities in children remains unknown.

The aim of the present study was to first investigate how cortical thickness covariance of language-related brain regions in preschoolers is associated with language comprehension abilities in the syntactic domain. In order to do so, we acquired structural magnetic resonance imaging (sMRI) data in 5-year-olds and applied a sentence picture-matching test with two syntactic conditions: 1) simple canonical subject-initial sentences and 2) syntactically complex non-canonical object-initial sentences (Schipke et al., 2012). Structural covariance mappings of cortical thickness were obtained by correlating the cortical thickness of the pre-defined language relevant seeds, that are, the left IFG and left posterior superior temporal gyrus/sulcus (pSTG/STS) (Friederici et al., 2011), to the rest of the cortex across individuals. Further, the relation of cortical thickness covariance mappings with sentence comprehension abilities of syntactically complex sentences in preschoolers was analyzed. Second, to be able to identify the developmental trajectory of cortical thickness covariance of language regions relevant for syntactic processing, we aimed to cross-sectionally compare cortical thickness covariance mappings of preschoolers, school age children, and adults. Thus, we additionally acquired sMRI data of school age children (9–13 years old) and adults (19–33 years old). Third, to demonstrate the agreement of cortical thickness covariance and white matter connectivity, we reconstructed white matter tracts between the left IFG and pSTG/STS using diffusion weighted imaging (DWI) data and compared the white matter tracts across development in relation to cortical thickness covariance mappings. Since DWI scanning parameters of school age children differed from preschool children and adults, we only compared white matter tracts in relation to cortical thickness covariance between preschool children and adults.

First, we expected that young preschool children display immature patterns of cortical thickness structural covariance of seeds that are specifically relevant for syntactic language processing (i.e., left IFG, left pSTG/STS), such that the seeds show covariance only with their contralateral homologous regions. Second, we expected that preschooler's cortical thickness covariance of language-relevant seeds was positively related to their ability to process syntactically complex non-canonical object-initial sentences (i.e., more mature left IFG to left pSTG/STS covariance in preschool children with enhanced language abilities). Third, in comparison to school age children and adults, we expected reduced structural coupling between the left IFG and STG in preschoolers. Fourth, we expected cortical thickness covariance mappings of the language-relevant seeds to develop in a similar way as the white matter tracts connecting the left IFG and left pSTG/STS.

2. Methods

2.1. Participants

A total number of 65 five-year-old preschool children (30 girls, *mean* age = 5.49 years, standard deviation (*SD*) = 0.28), 52 school age children in the age range of 9–13 years (23 girls, *mean* age = 10.37 years, *SD* = 0.59), and 53 adults in the age range of 19–35 years (22 females, *mean* age = 26.51 years, *SD* = 3.69) were included in the current study. The three groups were matched concerning gender ($\chi^2 = 0.26$, $p = 0.880$). Handedness was assessed using the modified version of Edinburgh Handedness Inventory (Oldfield, 1971). Preschoolers (right-handers: 60/65), school age children (right-handers: 48/52), and adults (right-handers: 53/53) did not differ significantly concerning their handedness ($p = 0.093$, *Fisher's Exact test*). For the children groups, non-verbal IQ was assessed by using the language-independent scale of the German version of the Kaufman Assessment Battery for Children (K-ABC, Kaufman and Kaufman, 1983). All children participants (i.e., preschoolers and school children) had a non-verbal IQ above 85, that is, within the normal range. For the adult group, the German intelligence test was used to measure non-verbal intelligence (Leistungs-Prüf-System, LPS, Horn, 1983); and they also fell into the normal range (i.e., >85). All participants were native German speakers, with no history of medical, psychiatric or neurological disorders. Written informed consent was obtained from all adult participants and the legal guardian or parent of the children; and children gave verbal assent for attendance before the experiments. The ethical review board of the University of Leipzig approved the study.

2.2. Behavioral language test

A sentence-picture matching test was administered outside the scanner to test preschool children's language comprehension abilities in the syntactic domain, which has been used in previous studies (Knoll et al., 2012; Schipke et al., 2012; Wu et al., 2016; Xiao et al., 2016). For the experiment, 24 sentences with subject-initial word order [i.e., simple canonical subject-initial sentences (SO)] and 24 sentences with object-initial word order [i.e., complex non-canonical object initial sentences (OS)] were used. All the used nouns were of masculine gender, as only in masculine nouns nominative and accusative can be unambiguously case-marked in German. In addition, we only used nouns of the strong declination type for which the preceding determiner already indicates the case. Thus, all nominal constituents in a sentence were unambiguously marked for accusative (ACC) or nominative (NOM). Sentence examples are as follows:

(1) SO
Der Tiger zieht den Igel.
[The tiger]$_{NOM}$ pulls [the hedgehog]$_{ACC}$.
The tiger pulls the hedgehog.

(2) OS
Den Igel zieht der Tiger.
[The hedgehog]$_{ACC}$ pulls [the tiger]$_{NOM}$.
The tiger pulls the hedgehog.

All items were presented auditorily - spoken by a trained female native speaker in a well-pronounced, child-directed manner. After each sentence, the child was presented with two pictures (Fig. 1), where one showed a scene corresponding to the sentence and the other served as a distractor. The child was then asked to point out the correct one out of the two pictures that were presented. Preschool children performed significantly above chance level on both SO sentences (accuracy: 94.29%, *SD*: 8.92, $t(64) = 40.05$, $p < 0.001$) and more complex OS sentences (accuracy: 77.12%, *SD*: 18.82, $t(64) = 11.61$, $p < 0.001$). In addition, scores on SO sentences were significantly higher than scores on OS sentences ($t(63) = 7.87$, $p < 0.001$), but they significantly correlated with each other ($r = 0.45$, $p < 0.001$).

Additionally, a standardized and norm-referenced language test (Test zum Satzverstehen von Kindern, TSVK, [English: sentence comprehension test], Siegmüller et al., 2011), assessing the general sentence comprehension abilities of children was administrated to ensure that children did not have general sentence comprehension difficulties. Of note, two preschoolers showed a *T score* below the average norm range of $T = 40$ to 60 (i.e., 32) and were thus excluded from further analyses.

2.3. Data acquisition

Both T1-weighted sMRI data and DWI data were collected on a Siemens 3T MRI scanner with a 12 channel array head coil. The high-resolution 3D T1-weighted magnetization prepared gradient-echo (MP-RAGE) image was acquired using following parameters: TI = 740 ms; TR = 1480 ms; TE = 3.46 ms; alpha = 10°; image matrix = 256 × 240; FOV = 256 × 240 mm^2; 128 sagittal slices; spatial resolution = 1 × 1 × 1.5 mm^3. Before the formal MRI scanning, children were asked to participate in a mock scan to familiarize with the environment and the experimental procedure.

DWI data were only available for 53 out of the 65 preschool children (*mean* age = 5.46, *SD* = 0.27; 24 girls) and 46 out of 53 adults (*mean* age = 26.30, *SD* = 3.66; 19 females), due to drop-out or large head motion. Again, there were no differences concerning gender ($\chi^2 = 0.16$, $p = 0.690$) and handedness ($p = 0.121$, *Fisher's Exact test*) distribution between the two age groups. Data were acquired using the twice-refocused spin echo echo-planar-imaging (EPI) sequence (TE = 83 ms; TR = 8 s; 100 × 100 image matrix; FOV = 186 × 186 mm^2; 66 axial slices (no gap); spatial resolution: 1.86 × 1.86 × 1.9 mm^3). Two sets of diffusion-weighted images were acquired: first, we scanned 60 isotropically distributed diffusion-encoding gradient directions with a *b*-value of 1000 s/mm^2, along an anterior-to-posterior phase encoding direction. Seven $b = 0$ s/mm^2 images were additionally acquired as anatomical reference and interleaved after each block of 10 diffusion-weighted

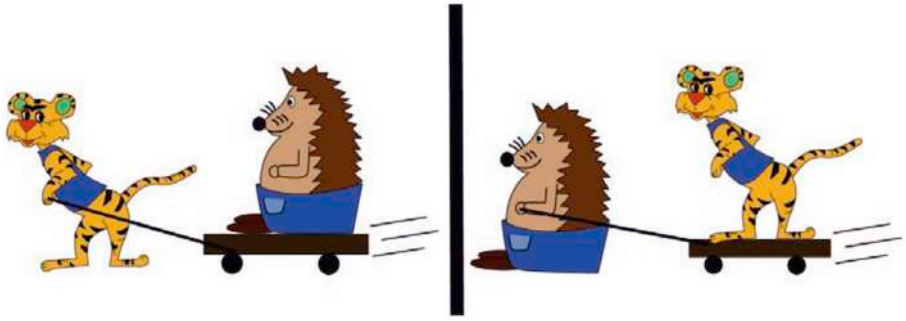

Fig. 1. Picture examples for the syntactic sentence comprehension ability test. Children were asked to choose whether the left or the right picture matched with the sentence they were presented with.

images for off-line motion correction. The second set was acquired along a posterior-to-anterior phase encoding direction, including one $b = 0$ s/mm^2 image and one $b = 1000$ s/mm^2 diffusion-weighted volume.

2.4. Data processing

2.4.1. sMRI data processing

Before processing, all T1-weighted images were visually inspected and their quality was further checked using the Computational Anatomy Toolbox (CAT12) (for more details, see http://dbm.neuro.uni-jena.de/vbm/check-sample-homogeneity). Cortical reconstruction and volumetric segmentation was performed using the FreeSurfer software, version 5.3.0 (http://surfer.nmr.mgh.harvard.edu/). The automatic processing procedure of FreeSurfer included skull stripping, gray-matter segmentation, cortical surface model reconstruction, and a number of deformation procedures, including surface inflation, registration to a spherical atlas, parcellation of the cerebral cortex, and creation of a variety of surface-based data (Dale et al., 1999; Fischl et al., 1999; Han et al., 2006). The reconstructed surfaces were visually inspected and manually edited for inaccuracies. The cortical thickness was calculated as the closest distance from the pial surface to the white matter surface at each vertex (Fischl and Dale, 2000). The vertex-wise thickness maps of individuals were aligned to Freesurfer *fsaverage* surface-based template, since it has been shown that using this template for children from ages 4 to 11 does not result in an age-associated bias (Ghosh et al., 2010). Finally, thickness maps were smoothed using a 20-mm full-width-at-half-maximum (FWHM) Gaussian Kernel.

2.4.2. Seed selection for cortical thickness covariance analysis

A seed-based analysis was conducted to examine the correlation between the cortical thickness in one seed and all the other vertices on the cortex across individuals (Bernhardt et al., 2014a; Lerch et al., 2006; Valk et al., 2016). The left IFG and pSTG/STS were selected as regions of interest (ROIs) according to previous functional MRI studies, where these two regions have been frequently reported to be involved in syntactic language processes, especially for syntactically complex sentences (Friederici et al., 2011; Xiao et al., 2016). Specifically, two seeds of the left hemisphere with the following talairach coordinates were used: [-53, 20, 15] (left IFG) and [-56, −43, 9] (left pSTG/STS) (Friederici et al., 2011; Xiao et al., 2016). These coordinates were mapped to the closest surface vertex on the FreeSurfer *fsaverage* template. The vertex-wise seed was subsequently defined as vertices within a sphere of a 5 mm radius around the coordinates. Right hemisphere homologous ROIs were also chosen (see Supplementary Materials for detailed results), because children demonstrate more inter-hemispheric activation during sentence processing in comparison to adults (Brauer et al., 2008; Brauer and Friederici, 2007; Holland et al., 2001). Additionally, the language-unrelated right primary visual cortex (V1) with MNI coordinates [9, −81, 7] as well as the right primary motor cortex, that is the right precentral gyrus [28, −16, 66], were selected as control seeds (Zielinski et al., 2010).

2.4.3. DWI data processing

DWI data was preprocessed using FSL (http://www.fmrib.ox.ac.uk/fsl) (Jenkinson et al., 2012; Smith et al., 2004; Woolrich et al., 2009). Volumes affected by motion artifacts were removed manually. Out of a total of 67 volumes, on average 1.06 volumes ($SD = 2.17$; maximum = 9) were removed for preschool children and 0.17 volumes ($SD = 0.57$; maximum = 3) were removed for adults. Preschool children and adults differed significantly concerning the number of removed volumes ($t = 2.68, p < 0.009$). Motion was estimated using the first reference $b = 0$ image and rigid-body registration. Diffusion-weighted images were rigidly aligned to their skull-stripped T1-weighted brain, which were generated during FreeSurfer reconstruction and co-registered to the standard Montreal Neurological Institute standard space (MNI 152) using flirt implemented in FSL. Distortion correction was performed by incorporating shift maps and the estimated head motion correction to unwarp the data. All transformations were combined before application so that data was interpolated only once. Diffusion tensor was fit to each voxel and FA along with axial diffusivity (AD), radial diffusivity (RD), and mean diffusivity (MD) maps were derived. AD measures the major eigenvector of the tensor, which is parallel to the tissue fiber. RD represents the two shortest eigenvalues, which is perpendicular to fibers. MD can be defined as the average of the three eigenvalues (Alexander et al., 2011).

Probabilistic tractography was then performed using FSL's typical processing pipeline (Behrens et al., 2007, 2003). The probabilistic distribution of fiber orientations from each voxel was estimated with a two-tensor model. Two surface-based ROIs used in the cortical thickness covariance analysis were also used as seeds in the tractography analysis (i.e., left IFG, left pSTG/STS). The detailed ROI transformation is described in the Supplementary Materials. Individual white matter masks were generated by thresholding FA maps with FA > 0.15. Probabilistic tractography was conducted in the individual space between the two ROIs within the white matter mask. In order to obtain the total connectivity between the target and seed region, we swapped seed and target to perform the tractography twice. The final reconstructed streamlines were computed as the sum of resulting streamlines of the two tractography processes (Patterson et al., 2014).

The number of streamlines (NOS) between the two ROIs was computed during tractography. To correct the seed volume effect on the NOS, streamline density, reflecting the connectivity strength, was first defined as a normalized version of NOS using:

$$StreamlineDensity = \frac{log(NOS)}{log(N \times V_{seed})}$$

where N refers to the number of sample streamlines in each seed voxel (here, N = 5000) and V_{seed} the number of voxels within the seed (Müller-Axt et al., 2017). The logarithmic scaling used here ensures a normal distribution of the streamline density across participants. Second, voxel-based tractography images (in which the value of each voxel represents the number of streamlines that the voxel contains) were also normalized in the same way to correct for seed size. A group mask of tracts between the two ROIs was created for visualization purposes, setting those voxels for which at least 50% of subjects showed non-zero values to 1, and otherwise to 0 within both groups of children and adults. Finally, the average values of FA, AD, RD, and MD of the IFG-to-pSTG/STS tract were obtained for each individual.

2.5. Statistical analyses

The Surfstat toolbox (http://www.math.mcgill.ca/keith/surfstat/) was used for the vertex-wise structural covariance analyses. Before analyses, we checked for outliers both within and across groups. For each participant, the mean thickness of the whole cortex was within the range of 3 *SD* compared to the mean of either the corresponding age group or of the whole sample. Thus, no participant was excluded for further analyses. In each model, age, gender, and handedness were added as covariates for within-group analyses, while only gender and handedness were added as covariates for between-group comparisons. Furthermore, total brain volume (TBV) was added as a covariate to control for the individual differences in brain volume across development. The seed-based structural covariance mapping for each vertex i on its cortical thickness Y_i was obtained for each age group separately using the following model:

$$Y_i = 1 + \text{Age} + \text{Gender} + \text{TBV} + \text{Seed} + \text{Handedness}$$

To examine the association between cortical thickness covariance and individual differences in language performance (i.e., LAN = language relevant behavioral tests) for preschoolers, the following model was applied for each vertex i on its cortical thickness Y_i:

$$Y_i = 1 + Age + Gender + TBV + Seed + LAN + Seed \times LAN + Handedness$$

To ensure that the associations between cortical thickness covariance and language performance was specific to language, IQ was additionally controlled for, by adding it as a covariate. To assess the developmental effect on thickness covariance mapping, we used the model including the parametric interaction between seed and group, that is:

$$Y_i = 1 + Gender + TBV + Seed + Group + Seed \times Group + Handedness$$

Given that imbalanced group sizes can violate the homogeneity of variance assumption of analyses of variances (ANOVAs), *Levene's* test was conducted, showing that our data met the criteria for homoscedasticity ($p = 0.812$, $F = 0.21$, $SD = 0.08$, 0.09 and 0.09 for adults, school age children and preschool children, respectively). In addition, the ratio of the largest variance to the smallest variance (i.e., should be less than 1.5) of groups can be used as a rule of thumb for judging the robustness of ANOVAs (Blanca et al., 2017; Ruscio and Roche, 2012). For the present data the variance ratio was 1.12, further justifying using parametric tests for the present data.

For white matter connectivity, two-sample *t* tests were performed to examine the developmental changes of streamline density, FA, AD, RD, and MD between preschool children and adults. As children and adults differed significantly concerning the total number of removed volumes, we added the number of removed volumes as a covariate to control for image quality differences between groups. Meanwhile, gender and handedness were also included as covariates. In order to examine the relationship between structural covariance and white matter connectivity, the association between the seed-based cortical thickness covariance and DWI measures (i.e., streamline density, FA, AD, RD, and MD) for each age group was calculated by including the parametric interaction between seed thickness and DWI measures using the following model for each vertex *i* on its thickness Y_i:

$$Y_i = 1 + Age + Gender + TBV + Handedness + DWI\ measures + Seed + Seed \times DWI\ measures$$

In addition, mean FA (or mean of other DWI measures) of the whole-brain, and the number of removed volumes was used as covariates. If not otherwise specified, a cluster-forming threshold of $p < 0.005$ was used, since this threshold ensures a false positive rate below 5% for thickness analyses as discussed by Greve and Fischl (2018). All surface-based results were thresholded at a cluster level $p < 0.05$ (two-tailed) corrected for multiple comparisons based on random field theory (Worsley et al., 1999).

3. Results

3.1. Seed-based cortical thickness covariance in preschoolers

The seed-based structural covariance mapping of cortical thickness was obtained first for preschoolers (Fig. 2 and Supplementary Table S1). We found that the left IFG only showed significant cortical thickness covariance with its surrounding area and the right IFG in the preschool children. Further, the left pSTG/STS was observed to structurally co-vary with proximal regions of the left pSTG/STS as well as with the bilateral middle temporal gyrus (MTG), bilateral inferior parietal lobule (IPL), left supramarginal gyrus (SMG), and right inferior temporal gyrus (ITG) in preschool children. Cortical thickness covariance of the right-hemispheric seeds was found to show similar patterns as in the left hemisphere. Specifically, the right IFG showed a strong co-variation with the seed itself and with its neighboring regions, as well as with the contralateral homologues regions. In contrast, the right pSTG/STS only showed co-variation with the seed itself and with its neighboring regions (see Supplementary Fig. S1).

3.2. Association between cortical thickness covariance and language abilities in preschoolers

We continued to examine whether cortical thickness covariance of our ROIs was associated with language abilities in preschool children. Cortical thickness covariance seeding from the left IFG showed a positive association with performance on the object-initial sentence (uncorrected $p < 0.001$), which does not survive correction for multiple comparison. However, when using a more liberal, but typically used cluster-forming threshold for surface-based thickness data, $p < 0.025$ (Greve and Fischl, 2018; Valk et al., 2017), we found a positive association between the left IFG and left temporal structural covariance and performance on the OS sentences with IQ included as an additional covariate ($p < 0.010$, Fig. 3A, FWE-corrected), which survives correction for multiple comparison. This positive association indicates increased left inferior frontal to temporal covariance to be related to higher abilities in processing object-initial sentences in preschoolers. To further explore the association between cortical thickness covariance and language performance, preschoolers were split into two subgroups (i.e., high- and low-performing children) by the median of performance scores regarding OS sentences. High-performing children (*mean* accuracy = 90.83%, $SD = 5.23$) showed significantly higher accuracy ($t = 10.61$, $p < 0.001$) in comparison to low-performing children (*mean* accuracy = 60.12%, $SD = 16.13$). Concerning their IQ scores, the two subgroups did not show any significant differences (*mean* = 107.63, $SD = 8.24$, for high-performing children; *mean* = 109.50, $SD = 10.00$, for low-performing children; $t = 0.81$, $p = 0.418$). When comparing the low- and high-performing group of preschoolers concerning their cortical thickness covariance, we found significant group differences ($p = 0.005$, Fig. 3B, FWE-corrected). Specifically, high-performing preschool children showed a positive covariance in cortical thickness between the left IFG seed and the peak value of the left temporal regions as target regions, while low performing preschool children demonstrated a negative covariance (Fig. 3C). Of note, after regressing out the covariates, one subject was noticed to be an outlier according to the residuals. However, when we removed this subject from the analysis, our results still remained significant (See Supplements 3 and Fig. S2). In addition, our procedure of splitting the group of preschoolers into two groups led to a reduction in sample size

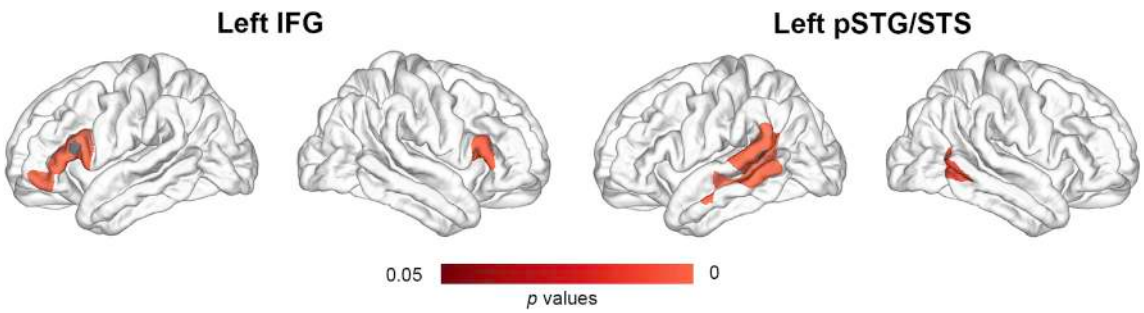

Fig. 2. Cortical thickness covariance maps seeding from the left IFG (left part of the Figure) and the left pSTG/STS (right part of the Figure) in preschool children. Only neighboring and contralateral homologous regions co-varied with the seed (depicted in gray) in preschoolers ($p < 0.05$, FWE-corrected at cluster level).

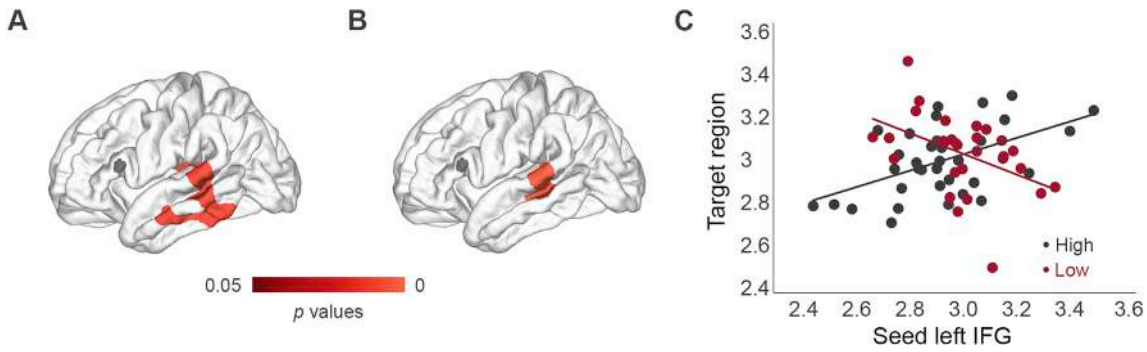

Fig. 3. Positive association between cortical thickness covariance seeding from the left IFG and preschoolers' sentence comprehension abilities of syntactically complex sentences. (A) Positive association between object-initial sentence abilities and cortical thickness covariance between the left IFG seed (depicted in gray) and the left temporal regions as target regions, including the left STG, MTG and ITG ($p < 0.010$). (B) Cortical thickness covariance differences between children with higher and children with lower sentence comprehension performance ($p = 0.005$, all FWE-corrected). (C) Positive covariance was found between the left IFG seed and the left temporal regions as target (peak value adjusted for model) in high-performing children ($r = 0.52$, $p = 0.003$, $t\,(29) = 3.27$; depicted in black), but a reversed negative covariance in low-performing children ($r = -0.41$, $p = 0.045$, $t\,(22) = -2.12$; depicted in red).

and, thus, a reduction in power. Thus, we obtained effect size maps for which the effect sizes on the significant cluster was Cohen's $d = 0.820$, indicating a large effect (See Supplementary Fig. S3). Together, these findings suggest that high-performing children are more likely to show the adult-like structural covariance of language relevant seeds (i.e., left IFG and left temporal regions) compared to low-performing children, which is independent of IQ. To confirm that intra-hemispheric covariation of the left IFG and left temporal regions, thought to be relevant for language processing, increases with development, we further compared cortical thickness covariance of preschool children with school age children and adults.

3.3. Group comparison of cortical thickness covariance across age groups

The seed-based cortical thickness covariance mapping of the left IFG and the left pSTG/STS was obtained for school age children and adults (see Figs. 4 and 5, respectively and Table S1). The left IFG (Fig. 4A) showed cortical thickness covariance with more extensive frontal regions, including bilateral middle frontal gyrus (MFG), superior frontal gyrus (SFG), bilateral precentral and postcentral gyrus, as well as temporoparietal regions, including left temporal and right parietal regions in school age children; and with more distant posterior regions in adults. Meanwhile, the significant co-varied region of the left pSTG/STS (Fig. 5A) seed extended to the left anterior temporal regions and the right SFG and precentral gyrus in school age children, and to more distant bilateral frontal regions and parietal regions in adults. Together with the cortical thickness covariance mapping in preschoolers, these findings suggest that cortical regions structurally co-vary with the selected language-relevant seeds demonstrating a progressive expansion during development.

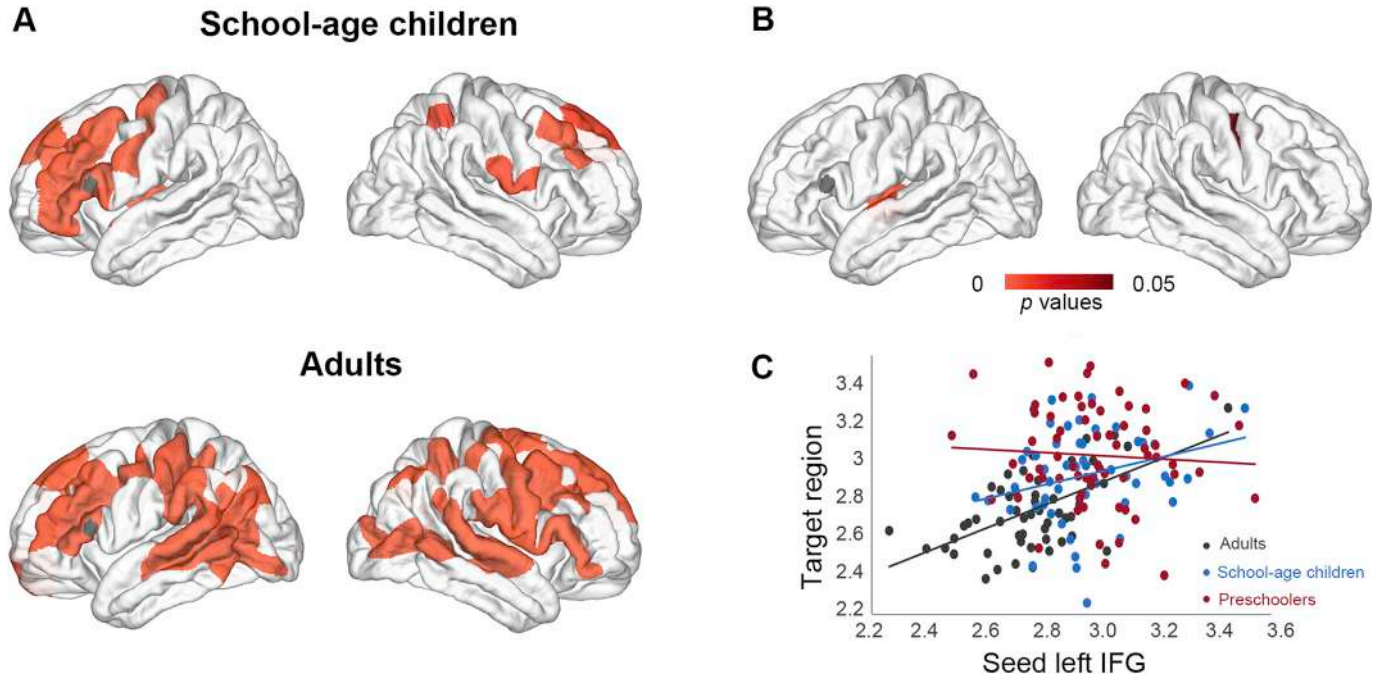

Fig. 4. Developmental differences on cortical thickness covariance maps seeding from the left IFG across age groups. (A) Cortical thickness covariance maps seeding from the left IFG (depicted in gray) in school age children (top) and adults (bottom). (B) Developmental differences for the cortical thickness covariance seeding from the left IFG across the three age groups. Significant differences were observed in the left temporal regions ($p = 0.006$) and the right precentral gyrus ($p = 0.043$, FWE-corrected). (C) Covariance of the left IFG seed and the left temporal regions as target (peak value adjusted for model) for all three age groups ($t\,(48) = 4.45$, $r = 0.54$, $p < 0.001$, for adults, in black; $t\,(47) = 1.98$, $r = 0.28$, $p = 0.053$, for school age children, in blue; $t\,(60) = -1.56$, $r = -0.20$, $p = 0.125$, for preschool children, in red).

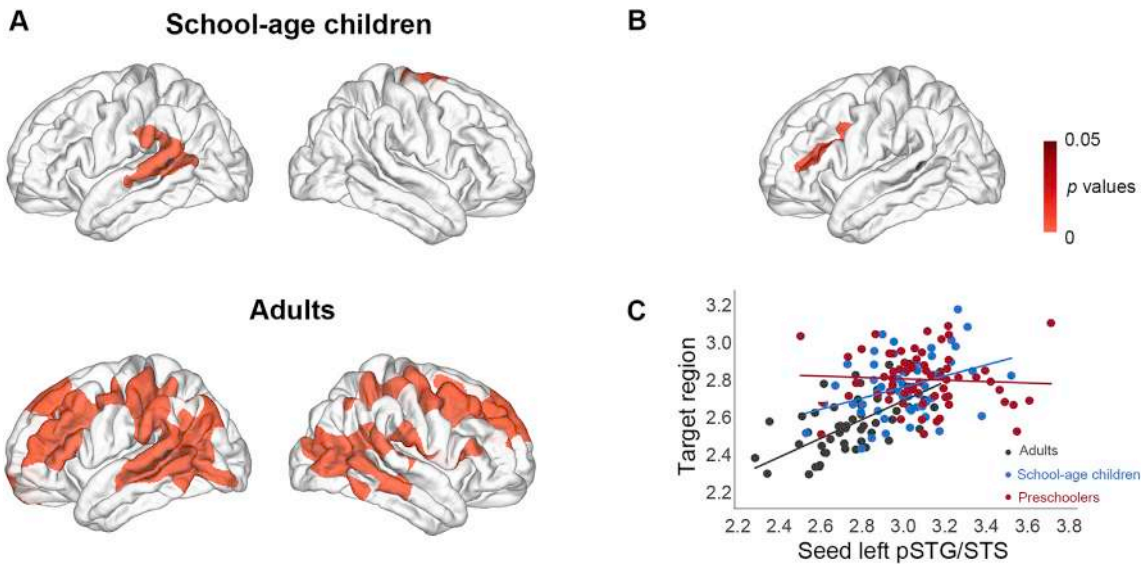

Fig. 5. Developmental differences on cortical thickness covariance maps seeding from the left pSTG/STS across age groups. (A) Cortical thickness covariance maps seeding from the left pSTG/STS (depicted in gray) in school age children (top) and adults (bottom). (B) Developmental differences for the cortical thickness covariance seeding from the left pSTG/STS across the three age groups. Significant differences were observed in the left frontal regions ($p = 0.006$, FWE-corrected). (C) Covariance of the left pSTG/STS seed and the left frontal regions as target (peak value adjusted for model) for all three age groups ($t\ (48) = 5.19$, $r = 0.60$, $p < 0.001$, for adults, in black; $t\ (47) = 2.60$, $r = 0.35$, $p = 0.012$, for school age children, in blue; $t\ (60) = -0.49$, $r = -0.06$, $p = 0.628$, for preschool children, in red).

We next statistically examined how cortical thickness covariance changes across age groups for the left IFG seed and the left pSTG/STS seed (see Figs. 4 and 5, respectively and Table 1). The direct group comparisons for the cortical thickness covariance centered on the left IFG seed across the three age groups revealed differences in the left superior temporal regions ($p = 0.006$) and the right precentral gyrus ($p = 0.043$) (Fig. 4B). Intriguingly, significant positive cortical thickness covariance was found between the thickness of the left IFG seed and the left superior temporal regions as target in adults ($t\ (48) = 4.45$, $r = 0.54$, $p < 0.001$). For school age children, we found a marginally significant positive covariance between the thickness of the left IFG seed and the left superior temporal regions as target ($t\ (47) = 1.98$, $r = 0.28$, $p = 0.053$), but we did not find a significant effect in preschoolers ($t\ (60) = -1.56$, $r = -0.20$, $p = 0.125$) (Fig. 4C). The post-hoc analysis further revealed that the group differences were driven by higher cortical thickness covariance between the left IFG seed and left superior temporal regions and insula ($p = 0.003$), as well as the covariance with the right precentral gyrus ($p = 0.003$) in adults as compared to preschool children (Table 1). Increased cortical thickness covariance between the left IFG seed and the left insula and a small patch of the temporal region ($p = 0.001$), and the right precentral gyrus ($p = 0.029$, all FWE-corrected) was also revealed in school children in comparison to preschool children. No significant cortical thickness covariance differences were observed between adults and school age children.

For the cortical thickness covariance seeding from the left pSTG/STS, significant differences were observed in a cluster located in the left frontal regions, including the left IFG, MFG, and precentral gyrus ($p = 0.006$) (Fig. 5B and Table 1). As illustrated in Fig. 5C, cortical thickness between the left pSTG/STS seed and the peak vertex of the significant target region, here IFG, exhibited no correlation in preschool children ($t\ (60) = -0.49$, $r = -0.06$, $p = 0.628$), but significant positive correlations in school age children ($t\ (47) = 2.60$, $r = 0.35$, $p = 0.012$) and adults ($t\ (48) = 5.19$, $r = 0.60$, $p < 0.001$). The post-hoc analysis further showed significantly higher cortical thickness covariance between the left pSTG/STS and left IFG (extending to MFG, precentral gyrus) in adults as compared to preschool children ($p < 0.001$) (Table 1). Further, school age children showed increased cortical thickness covariance between the left pSTG/STS seed and the left MFG and the left IFG in comparison to preschoolers ($p = 0.046$). Significant differences were also observed between school age children and adults in the left MFG and precentral gyrus ($p = 0.016$). The cortical thickness covariance for the right homologous seed centered on the right IFG did not reveal any significant differences between the three age groups, while the cortical thickness covariance seeding from the right STG/STS revealed developmental differences in the bilateral frontal regions ($p < 0.001$) and the right parietal regions ($p = 0.019$, all FWE-corrected) (see

Table 1
Developmental differences on the cortical thickness covariance between preschool children, school age children, and adults.

Seeds	Groups	Target regions	Cluster size	*p* values
Left IFG	Adults, school age, and preschool children	Left superiortemporal, insula, transversetemporal	2865	0.006
		Right precentral	1651	0.043
	Adults > preschool children	Left insula, superiortemporal, transversetemporal	1527	0.003
		Right precentral	939	0.003
	School age children > preschool children	Left insula, superiortemporal, transversetemporal	2180	0.001
		Right precentral	558	0.029
Left pSTG/STS	Adults, school age, and preschool children	Left parsopercularis, rostralmiddlefrontal, caudalmiddlefrontal, parstriangularis, precentral	2474	0.006
	Adults > preschool children	Left parsopercularis, rostralmiddlefrontal, caudalmiddlefrontal, parstriangularis, precentral	2405	<0.001
	Adults > school age children	Left caudalmiddlefrontal, precentral	404	0.016
	School age children > preschool children	Left rostralmiddlefrontal, parstriangularis	108	0.046

Supplements, Fig. S5A and Table S3).

3.4. Structural covariance mapping of cortical thickness for control regions

Cortical regions showing significant cortical thickness covariance with the right V1 were found to be similar in preschool children, school age children, and adults, with only neighboring areas to be co-varied (Fig. S4 and Table S2). Meanwhile, the right precentral gyrus seed was also revealed to be co-varied with similar cortical regions across three age groups, including bilateral precentral, SFG, paracentral gyrus, and right MFG, with the exception of the left inferior frontal region that was only revealed in adults (Fig. S4 and Table S2). Statistical comparisons across the three age groups showed significant differences in the surrounding areas of the seed, including the right postcentral, SMG, precentral gyrus, and inferior parietal lobule ($p = 0.004$, all FWE-corrected) (Fig. S5B and Table S3). These results indicate that the developmental trajectory of structural covariance that was found for the language-relevant seeds (i.e., left IFG and pSTG/STS) are specific, as we did not find them in the cortical thickness comparison of control seeds.

In addition, we examined the associations between language abilities and the structural covariance of control seeds in the preschool children to ensure that the found associations described above are specific to the language network. No significant group differences between low- and high-performers were found for the cortical thickness covariance seeding from the right V1 ($p = 0.068$) and the right precentral gyrus ($p = 0.798$, all FWE-corrected), which indicates that the association with language abilities was specific to the language-related cortical thickness covariance maps.

3.5. White matter tracts in preschool children and adults

We further examined whether the observed difference in the left IFG-to-pSTG/STS cortical thickness covariance between preschool children and adults was also reflected in the group's corresponding white matter connectivity. The connectivity strength between the left IFG and pSTG/STS, as measured by streamline density, was found to be significantly higher in adults than in preschool children. The FA of the connectivity between the left IFG and pSTG/STS was also observed to be significantly higher in adults than in preschool children. The AD, the RD, and the MD were significantly lower in adults than in preschooler (Fig. 6A and Table 2).

To illustrate the fiber tract between the left IFG and left pSTG/STS in preschool children and adults, a tract that existed in more than half of the subjects was obtained, separately for adults and preschool children (Fig. 6B). Our findings suggest an insufficiency in white matter tracts linking the left IFG and pSTG/STS in preschool children as compared to adults, which was in a line with the observed absence in thickness covariance between the left IFG and temporal regions in preschool children. When linking white matter measurements (i.e., streamline density, FA, AD, RD, MD between left IFG and pSTG/STS) to gray matter cortical thickness covariance, we only noted a positive association of FA with gray matter structural covariance between left pSTG/STS and left frontal regions (i.e., MFG, precentral, and IFG) in adults ($p = 0.013$, FWE-corrected) (Fig. 6C), but not in preschool children.

4. Discussion

In the present study, we investigated how cortico-cortical thickness covariance is associated with the syntactic processing abilities of preschool children, as well as how the syntax-related gray matter structural covariance pattern of cortical thickness develops from preschool children to adults. By computing cortical thickness covariance of two language-associated seeds (i.e., left IFG and left STG/STS), we found restricted covariance with the anatomically proximal and contralateral

Table 2
Descriptive and inference statistical information of diffusion weighted imaging parameters in preschoolers and adults.

DWI parameters	Preschoolers (*mean, SD*)	Adults (*mean, SD*)	Significance	
			t	*p*
Streamline density	0.42 (0.08)	0.51 (0.09)	4.26	$p < 0.001$
FA	0.39 (0.02)	0.41 (0.02)	4.70	$p < 0.001$
AD (mm/s^2)	1.16×10^{-3} (0.03×10^{-3})	1.08×10^{-3} (0.02×10^{-3})	−10.60	$p < 0.001$
RD (mm/s^2)	0.64×10^{-3} (0.25×10^{-3})	0.58×10^{-3} (0.24×10^{-3})	−9.52	$p < 0.001$
MD (mm/s^2)	0.82×10^{-3} (0.02×10^{-3})	0.75×10^{-3} (0.02×10^{-3})	−11.06	$p < 0.001$

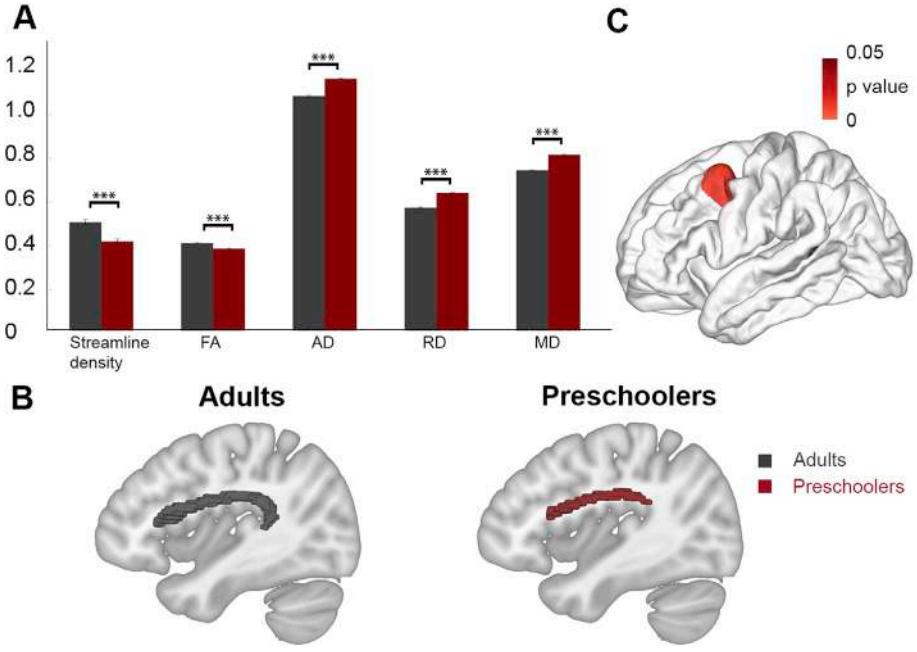

Fig. 6. Combination of gray matter structural covariance and white matter tractography in adults and preschool children. (A) Group differences in DWI measurements (i.e., streamline density, FA, AD ($\mu m/s^2$), RD ($\mu m^2/s$), and MD ($\mu m^2/s$); *** indicates $p < 0.001$). (B) For visualization purposes, the tracts that existed in more than half of the subjects were obtained separately for adults (left) and preschoolers (right) to illustrate the connectivity between the left IFG and the left pSTG/STS. (C) Positive association ($p = 0.013$, FWE-corrected) between the cortical thickness covariance and white matter tractography between the left frontal regions and the left pSTG/STS (depicted in gray) in adults.

homologous regions in young preschoolers. However, a more adult-like cortical thickness covariance between the left IFG and the left temporal regions was observed in those preschool children with enhanced syntactically complex sentence comprehension. These findings suggest that children with superior sentence comprehension abilities are more likely to show an adult-like pattern with stronger cortical thickness covariance in the inferior frontal and temporal circuit compared to children with reduced syntactic abilities. By further comparing cortical thickness covariance of preschool children with school age children and adults, we could show that the cortical thickness covariance pattern from the language-associated seeds develops progressively from very restricted to widely-distributed brain regions across the three age groups, with school age children showing a similar covariance pattern like adults, but preschoolers did not. Such trend was not observed for the cortical thickness networks of the control seeds. In addition, we could show that the difference of IFG-to-STG/STS cortical thickness covariance between preschoolers and adults was accompanied by distinctions in the white matter tracts linking these two areas, as reflected in streamline density, FA, AD, RD, and MD of the arcuate fasciculus. Further, we only found an association between cortical thickness covariance and white matter tracts linking the left IFG and left STG/STS in adults, but not yet in preschoolers. Together, these findings support our hypothesis that in comparison to adults, preschool children display immature patterns of gray matter structural covariance with reduced couplings between the left IFG and left STG. However, those preschoolers with enhanced sentence comprehension abilities showed more mature structural covariance patterns, that is, stronger cortical thickness covariance between the left IFG and left temporal regions.

4.1. Structural covariance mapping of cortical thickness in preschool children

In agreement with previous structural covariance studies in children (Geng et al., 2016; Zielinski et al., 2010), we showed a restricted structural covariance pattern of cortical thickness in the language network seeding from the left IFG and the left pSTG/STS that mainly co-varied with the neighboring and contralateral homologous regions in preschoolers, lacking long-range covariance between the left IFG and the left superior temporal cortex. These results suggest that the language network of young children has not fully developed, predominantly showing short-range and interhemispheric covariance. This is in line with findings showing that the network specialized for syntactic language processing develops gradually (Skeide and Friederici, 2016). Neuroimaging studies have shown that children between three and four years of age do not segregate syntactic from semantic processing at the neuroanatomical level, indicated by overlapping functional activation of similar regions for both processes. Although nine to ten year old children still do not show an adult-like complete selectivity in the left BA44, they begin to have selective activations in the left pSTG for syntactic processing in sentence comprehension (Brauer and Friederici, 2007; Nunez et al., 2011; Skeide et al., 2014; Skeide and Friederici, 2016). Further and also in line with our results, functional connectivity studies demonstrated stronger inter-hemispheric connectivity between the bilateral IFG rather than long-range intra-hemispheric connectivity between the left IFG and left pSTG in preschoolers compared to adults (Friederici et al., 2011; Xiao et al., 2016). This covariance or connectivity between the left frontal and temporal regions increases with age in young childhood and adolescence (Lerch et al., 2006; Vissiennon et al., 2017). Thus, by using structural covariance analysis, we confirm that the network specialized for syntactic processing has not fully developed in preschool children yet.

In general, dynamic causal modeling showed that the left IFG in its interaction with the posterior temporal regions plays a primary role during syntactic processing (den Ouden et al., 2012); and this default language functional network has been suggested to subserve complex sentence comprehension in adults (for reviews see Friederici, 2011, 2012). Interestingly, we observed a positive correlation between preschoolers' ability to process syntactically complex object-initial sentences and the structural covariance between left IFG seed and left temporal regions. More specifically, we could show that preschool children with enhanced sentence comprehension abilities are more likely to show stronger covariance in the inferior frontal and temporal cortex compared to children with reduced sentence comprehension abilities. Noteworthy, this positive correlation was not affected by general cognitive abilities (i.e., IQ), which implies that the cortical thickness covariance between the left frontal and temporal regions was specific to preschooler's syntactic sentence comprehension abilities. Importantly, the syntactic sentence comprehension abilities were only associated with the structural covariance of the language-related seeds, rather than with the control seed (e.g., right V1). Our findings of the specific positive correlation between cortical thickness covariance of language-related seeds and syntactic language abilities are in line with previous functional imaging studies that revealed a positive correlation between syntactic processing capacities and the functional activation in left perisylvian regions in young children (Knoll et al., 2012; Wu et al., 2016). Additionally, the functional connectivity between the left IFG and pSTG/STS was observed to be positively associated with the ability to process syntactically complex object-initial sentences in preschoolers (Xiao et al., 2016). Furthermore, the microstructure of the dorsal language pathway was also found to be correlated with sentence comprehension accuracy and speed in children from the ages between three to ten years (Skeide et al., 2016). Taken together, although preschool children mainly showed a restricted and inter-hemispheric covariance pattern, children with enhanced syntactic abilities show a stronger long-range intra-hemispheric covariance pattern between the left IFG and left temporal cortex that is thought to be the more adult-like covariance pattern.

4.2. Developmental changes of cortical thickness covariance from preschool children to adults

To confirm our assumption that preschool children with enhanced syntactic abilities indeed show a more adult-like cortical thickness covariance pattern (i.e., long-range covariance between the left IFG and left temporal cortex), we cross-sectionally compared cortical thickness covariance mappings of preschoolers with school age children and adults. We could show a linear developmental trajectory for the covariance between the seed (i.e., left IFG and left pSTG/STS) and target regions (i.e., left temporal and left frontal regions for each seed, respectively), from no covariance in preschoolers to high positive covariance in adults. In contrast to preschoolers, adults showed a distributed cortical thickness covariance pattern for the syntactic language network seeding from the left IFG and the left pSTG/STS. More specifically, we found long-range cortical thickness covariance between frontal and temporal regions. This finding is in line with previous structural covariance studies, showing a co-variation of BA44 as a seed with the posterior STG, fronto-parietal sensorimotor and cingulate motor areas in late adolescents; and a co-variation of the left temporal pole as a seed with temporal, insular, and frontal regions in late adolescents (Zielinski et al., 2010). Further, the here found structural covariance pattern is in line with the functional fronto-temporal language networks consistently found in adults (Fedorenko and Thompson-Schill, 2014; Friederici, 2012, 2011; Lohmann et al., 2010; Tomasi and Volkow, 2012). Thus, adults show a stronger fronto-temporal cortical thickness covariance in the syntactic language network, compared to preschoolers, suggesting a developmental tendency from local and inter-hemispheric to distant and intra-hemispheric cortical thickness covariance during language development (Fair et al., 2009, 2007; Kelly et al., 2009; Stevens et al., 2009; Supekar et al., 2009).

Our finding on the development of the cortical thickness covariance between brain regions relevant for syntactic processing is compatible with previous language-related structural covariance studies. For

example, the covariance between the left frontal and superior temporal regions increases with advancing age in adolescents in various language networks, such as the speech and semantic network (Lerch et al., 2006; Zielinski et al., 2010). Further, our results on the structural covariance are compatible with findings on developmental differences between adults and children in previous functional and white matter connectivity studies (Brauer and Friederici, 2007; Friederici et al., 2011; Skeide et al., 2016; Xiao et al., 2016). In particular, increased functional connectivity between frontal and temporal region has been found in adults, while children rather predominantly show interhemispheric functional connectivity, such as a connectivity between the left and right STG (Brauer and Friederici, 2007; Friederici et al., 2011; Xiao et al., 2016). Network studies further revealed decreased local network efficiency, but increased global network efficiency in white matter connectivity during development (Dennis et al., 2013; Gong et al., 2009; Hagmann et al., 2010). This tendency might be due to the continuous development of neural substrates that allow for more effective long-range neural pathways by intensifying co-activation between distant regions and weakening co-activation between locally aligned regions (Fair et al., 2009; Hagmann et al., 2010).

4.3. Convergence of gray and white matter network

In order to further support our assumption that long-range neural pathways are immature in preschool children and, thus, might be one reason for their reduced structural covariance, we reconstructed white matter tracts between the left IFG and pSTG/STS in preschool children and compared them with those of adults. As expected, we found superior connectivity strength (i.e., measured by streamline density) and white matter maturation status (i.e., measured by FA, AD, RD, and MD) of the arcuate fasciculus in the mature brain compared to the immature brain. Our developmental changes of the DWI parameters are generally in line with previous findings. Specifically and in line with several other studies, we found an increase of FA when comparing children with adults, such that adults show higher FA values compared to children (Krogsrud et al., 2016; Kumar et al., 2012; Lebel et al., 2012, 2008; Lebel and Beaulieu, 2011; Schmithorst et al., 2002; Yeatman et al., 2014). In contrast MD and RD were shown to decrease from childhood to adulthood (Krogsrud et al., 2016; Kumar et al., 2012; Lebel et al., 2012; Westlye et al., 2010; Yeatman et al., 2014), which we also observed in the present study. Of note, we also observed a decrease of AD with age. Concerning the maturation of AD, however, research has shown an equivocal picture (for reviews see, Yap et al., 2013). Several studies suggested that AD increases with age in adolescents (Ashtari et al., 2007; Bava et al., 2010) and older adults (Barrick et al., 2010), which is in contrast to our findings. However, others suggested that AD decreases from childhood to adulthood in the whole brain (Eluvathingal et al., 2007; Hsu et al., 2010; Krogsrud et al., 2016; Kumar et al., 2012; Tamnes et al., 2010) and particularly in the arcuate fasciculus (Eluvathingal et al., 2007), which is in line with the present results. The differential changes of DWI measures across development might be explained by substantial microstructural changes differently influencing DWI measures. Generally, it is assumed that RD measures diffusion of water perpendicular to fibers, indicating myelination, while AD measures water diffusion parallel to tissue fibers, indicating axonal status or extra axonal/cellular space change (Beaulieu, 2002; Song et al., 2005, 2002; Suzuki et al., 2003). Thus, the observed age-related increase of FA, but decrease of MD, both discussed to be summary measures of AD and RD (Alexander et al., 2011), might be driven by an age-related increase in myelination (Silbereis et al., 2016) as indicated by RD. This further goes along with an increased number of fibers or increased axonal caliber, which then allows fibers to become less straight due to reduced inter axonal/cellular space, as indicated by decreased AD (Kumar et al., 2012; Mukherjee and McKinstry, 2006; Qiu et al., 2008; Suzuki et al., 2003). Further corresponding to our results, the white matter dorsal pathway has been observed to be less mature in children at the age of seven (Brauer et al., 2013, 2011; Lebel et al., 2008; Zhang et al., 2007). In addition, adults were shown to have increased FA of the dorsal arcuate fasciculus compared with children even at the ages of nine to ten years (Skeide et al., 2016).

Moreover and importantly, we also found an association between the cortical thickness covariance and the FA of the white matter tracts linking the left IFG and left STG/STS in adults, but not yet in preschoolers. As stated above, FA can be described as a summary measure of white matter microstructural properties, such as axonal myelination, packing density and membrane permeability (Alexander et al., 2011; Beaulieu, 2002). Thus, the association between white matter tract and structural covariance in fronto-temporal regions might suggest that thickness covariance is mediated by white matter connectivity (Ferrer et al., 1995; Gong et al., 2012; Mechelli, 2005). Specifically, the mediation by white matter connectivity is most likely related to the white matter microstructural properties, such as myelination and axonal packing that were found to modulate FA (Alexander et al., 2011; Beaulieu, 2002). This hypothesis is further supported by the observation of associations between cortical thickness and myelination across development (Cafiero et al., 2018; Whitaker et al., 2016). Therefore, it might be suggested that the emergence of structural covariance between frontal and temporal regions with age, as demonstrated by the present study, was at least partially mediated by an increase in white matter connections across development.

However, next to white matter connections, we have to consider other factors that most likely influence the emergence of structural covariance. Another crucial factor for the underlying structural covariance might be functional connectivity of synchronous neuronal activation (Honey et al., 2010; Hosseini and Kesler, 2013). A direct functional and structural relationship was demonstrated by showing that the intrinsic functional connectivity and gray matter volume patterns converge in adults and children (Alexander-Bloch et al., 2013b; Seeley et al., 2009). In the present study, we did not directly combine functional with structural data. However, in line with the results of Xiao et al. (2016), we would expect that preschoolers show reduced intrinsic functional connectivity between the left IFG and pSTG compared to adults and to children with enhanced syntactic abilities. Further, gene expression was shown to influence the emergence of structural covariance in both animal and human cortices (Romero-Garcia et al., 2018; Schmitt et al., 2008; Yee et al., 2018). Thus, the neurobiological mechanisms that underlie structural covariance are complex, including white matter, functional connectivity, and gene expression. Taken together, when combining our results with above mentioned studies, we suggest that across development anatomically co-varied regions become more likely functionally connected, which is sustained and mediated by white matter connectivity and gene expression (Alexander-Bloch et al., 2013a,b; Gong et al., 2012; Yee et al., 2018), possibly as a function of improving language abilities.

4.4. Functional specialization of cortical thickness covariance from preschool children to adults

To analyze whether the emergence of structural covariance depends on its functional specialization, we additionally analyzed the cortical thickness covariance of the control regions (i.e., the lower order networks right V1 and right precentral gyrus) cross-sectionally across the three age groups. Both control regions demonstrated stable covariance patterns with slight differences for the right precentral gyrus across groups (but not for the visual network, V1), such that adults demonstrated higher covariance with the neighboring regions of the right precentral gyrus as a seed in comparison to children. Thus, our results suggest two alternative developmental trajectories for different cognitive functions, which are in line with previous life-span studies (Li et al., 2013; Montembeault et al., 2012; Zielinski et al., 2010). Over and above, these differential structural covariance patterns of high- and low-order seeds might indicate that the evolvement of structural covariance networks depends on the developmental trajectory of their functional specialization, such that lower-order networks evolve earlier in development, but the higher-order language

network develops later during childhood (see also Zielinski et al., 2010, for similar results on the higher order default mode and control network).

4.5. Limitations and future directions

Several limitations should be considered. First, the cross-sectional design of our study underestimates the changes within individuals over time. Therefore, longitudinal studies are required to sufficiently examine the dynamic trajectory of the brain's structural covariance during development (Raznahan et al., 2010). Second, we only assessed preschooler's syntactic sentence comprehension abilities in association with cortical thickness covariance of ROIs reported to be involved in syntactic language processes. Future studies in addition analyzing cortical thickness covariance in association with other language competences, such as phonological and semantic abilities, may gain a deeper understanding of the development of the cortical thickness covariance of networks associated with language processing. Moreover, due to the absence of behavioral tests for school age children and adults, we were not able to investigate language abilities in relation to structural covariance in the other two age groups, which would have further supported our claim that the development of the long range intra-hemispheric fronto-temporal structural covariance of the syntactic language network is associated with syntactic language abilities. Finally, our claim that structural covariance is associated with syntactic language abilities in preschoolers was based on a modest sample size. Although we could demonstrate large effect sizes, results should be verified in future studies using larger samples to enhance power.

5. Conclusion

In the current study, we demonstrate that the cortical thickness covariance pattern of brain regions relevant for syntactic processes develops from a less mature (i.e., co-varying with the contralateral homologous regions) in preschoolers to a more mature one (i.e., increasing long-range intra-hemispheric covariance) in school age children and adults. The structural covariance of cortical thickness between the left frontal and left temporal regions was shown to be positively related to the sentence comprehension abilities in preschool children. More specifically, cortical thickness covariance of children with enhanced syntactic abilities was demonstrated to be more adult-like, showing stronger cortical thickness covariance between the left frontal and temporal regions. Further, we showed an association between the gray matter structural covariance and the white matter connectivity between the left frontal and temporal regions in adults, but not yet in preschoolers. Thus, our study represents not only the characterization of the anatomical changes of the language network during development, but moreover, highlights its link to syntactic language comprehension abilities.

Acknowledgements

This work was funded by the German Research Foundation (project FR 519/20-1 (FOR 2253) awarded to A.D.F.) and by the Max Planck Society and the Fraunhofer Society (Grant number M.FE.A.NEPF0001).

T.Q. was finically supported by the China Scholarship Council (201506040035). We would like to thank Indra Kraft and Kodjo Vissiennon for collecting the data; Thomas C. Gunter and Clara Ekerdt (Max Planck Institute for Human Cognitive and Brain Sciences, Leipzig, Germany) for providing suggestions on our manuscript; and Yongbin Wei (VU Amsterdam, the Netherlands) for providing codes for brain mapping plot and helpful discussion on our work.

Appendix A. Supplementary data

Supplementary data to this article can be found online at https://doi.org/10.1016/j.neuroimage.2019.02.014.

References

Alexander-Bloch, A., Giedd, J.N., Bullmore, E., 2013a. Imaging structural co-variance between human brain regions. Nat. Rev. Neurosci. 14, 322–336. https://doi.org/10.1038/nrn3465.

Alexander-Bloch, A., Raznahan, A., Bullmore, E., Giedd, J., 2013b. The convergence of maturational change and structural covariance in human cortical networks. J. Neurosci. 33, 2889–2899. https://doi.org/10.1523/JNEUROSCI.3554-12.2013.

Alexander, A.L., Hurley, S.A., Samsonov, A.A., Adluru, N., Hosseinbor, A.P., Mossahebi, P., Tromp, D.P.M., Zakszewski, E., Field, A.S., 2011. Characterization of cerebral white matter properties using quantitative magnetic resonance imaging stains. Brain Connect. 1, 423–446. https://doi.org/10.1089/brain.2011.0071.

Ashtari, M., Cervellione, K.L., Hasan, K.M., Wu, J., McIlree, C., Kester, H., Ardekani, B.A., Roofeh, D., Szeszko, P.R., Kumra, S., 2007. White matter development during late adolescence in healthy males: a cross-sectional diffusion tensor imaging study. Neuroimage. https://doi.org/10.1016/j.neuroimage.2006.10.047.

Barrick, T.R., Charlton, R.A., Clark, C.A., Markus, H.S., 2010. White matter structural decline in normal ageing: a prospective longitudinal study using tract-based spatial statistics. Neuroimage. https://doi.org/10.1016/j.neuroimage.2010.02.033.

Bava, S., Thayer, R., Jacobus, J., Ward, M., Jernigan, T.L., Tapert, S.F., 2010. Longitudinal characterization of white matter maturation during adolescence. Brain Res. https://doi.org/10.1016/j.brainres.2010.02.066.

Beaulieu, C., 2002. The basis of anisotropic water diffusion in the nervous system - a technical review. NMR Biomed. https://doi.org/10.1002/nbm.782.

Behrens, T.E.J., Berg, H.J., Jbabdi, S., Rushworth, M.F.S., Woolrich, M.W., 2007. Probabilistic diffusion tractography with multiple fibre orientations: what can we gain? Neuroimage 34, 144–155. https://doi.org/10.1016/j.neuroimage.2006.09.018.

Behrens, T.E.J., Woolrich, M.W., Jenkinson, M., Johansen-Berg, H., Nunes, R.G., Clare, S., Matthews, P.M., Brady, J.M., Smith, S.M., 2003. Characterization and propagation of uncertainty in diffusion-weighted MR imaging. Magn. Reson. Med. 50, 1077–1088. https://doi.org/10.1002/mrm.10609.

Bernhardt, B.C., Klimecki, O.M., Leiberg, S., Singer, T., 2014a. Structural covariance networks of the dorsal anterior insula predict females' individual differences in empathic responding. Cerebr. Cortex 24, 2189–2198. https://doi.org/10.1093/cercor/bht072.

Bernhardt, B.C., Valk, S.L., Silani, G., Bird, G., Frith, U., Singer, T., 2014b. Selective disruption of sociocognitive structural brain networks in autism and alexithymia. Cerebr. Cortex 24, 3258–3267. https://doi.org/10.1093/cercor/bht182.

Blanca, M.J., Alarcón, R., Arnau, J., Bono, R., Bendayan, R., 2017. Effect of variance ratio on ANOVA robustness: might 1.5 be the limit? Behav. Res. Methods 1–26. https://doi.org/10.3758/s13428-017-0918-2.

Brauer, J., Anwander, A., Friederici, A.D., 2011. Neuroanatomical prerequisites for language functions in the maturing brain. Cerebr. Cortex 21, 459–466. https://doi.org/10.1093/cercor/bhq108.

Brauer, J., Anwander, A., Perani, D., Friederici, A.D., 2013. Dorsal and ventral pathways in language development. Brain Lang. 127, 289–295. https://doi.org/10.1016/j.bandl.2013.03.001.

Brauer, J., Friederici, A.D., 2007. Functional neural networks of semantic and syntactic processes in the developing brain. J. Cognit. Neurosci. 19, 1609–1623. https://doi.org/10.1162/jocn.2007.19.10.1609.

Brauer, J., Neumann, J., Friederici, A.D., 2008. Temporal dynamics of perisylvian activation during language processing in children and adults. Neuroimage 41, 1484–1492. https://doi.org/10.1016/j.neuroimage.2008.03.027.

Cafiero, R., Brauer, J., Anwander, A., Friederici, A.D., 2018. The concurrence of cortical surface area expansion and white matter myelination in human brain development. Cerebr. Cortex 29, 827–837. https://doi.org/10.1093/cercor/bhy277.

Dale, A.M., Fischl, B., Sereno, M.I., 1999. Cortical surface-based analysis: I. Segmentation and surface reconstruction. Neuroimage 9, 179–194. https://doi.org/10.1006/nimg.1998.0395.

den Ouden, D.B., Saur, D., Mader, W., Schelter, B., Lukic, S., Wali, E., Timmer, J., Thompson, C.K., 2012. Network modulation during complex syntactic processing. Neuroimage 59, 815–823. https://doi.org/10.1016/j.neuroimage.2011.07.057.

Dennis, E.L., Jahanshad, N., McMahon, K.L., de Zubicaray, G.I., Martin, N.G., Hickie, I.B., Toga, A.W., Wright, M.J., Thompson, P.M., 2013. Development of brain structural connectivity between ages 12 and 30: a 4-Tesla diffusion imaging study in 439 adolescents and adults. Neuroimage 64, 161–684. https://doi.org/10.1016/j.neuroimage.2012.09.004.

Draganski, B., Gaser, C., Busch, V., Schuierer, G., Bogdahn, U., May, A., 2004. Neuroplasticity: changes in grey matter induced by training. Nature 427, 311–312. https://doi.org/10.1038/427311a.

Eluvathingal, T.J., Hasan, K.M., Kramer, L., Fletcher, J.M., Ewing-Cobbs, L., 2007. Quantitative diffusion tensor tractography of association and projection fibers in normally developing children and adolescents. Cerebr. Cortex. https://doi.org/10.1093/cercor/bhm003.

Fair, D.A., Cohen, A.L., Power, J.D., Dosenbach, N.U.F., Church, J.A., Miezin, F.M., Schlaggar, B.L., Petersen, S.E., 2009. Functional brain networks develop from a "local to distributed" organization. PLoS Comput. Biol. 5 https://doi.org/10.1371/journal.pcbi.1000381.

Fair, D.A., Dosenbach, N.U.F., Church, J.A., Cohen, A.L., Brahmbhatt, S., Miezin, F.M., Barch, D.M., Raichle, M.E., Petersen, S.E., Schlaggar, B.L., 2007. Development of distinct control networks through segregation and integration. Proc. Natl. Acad. Sci. Unit. States Am. 104, 13507–13512. https://doi.org/10.1073/pnas.0705843104.

Fedorenko, E., Behr, M.K., Kanwisher, N., 2011. Functional specificity for high-level linguistic processing in the human brain. Proc. Natl. Acad. Sci. U. S. A 108, 16428–16433. https://doi.org/10.1073/pnas.1.

Fedorenko, E., Thompson-Schill, S.L., 2014. Reworking the language network. Trends Cognit. Sci. https://doi.org/10.1016/j.tics.2013.12.006.
Fengler, A., Meyer, L., Friederici, A.D., 2015. Brain structural correlates of complex sentence comprehension in children. Dev. Cogn. Neurosci. 15, 48–57. https://doi.org/10.1016/j.dcn.2015.09.004.
Ferrer, I., Blanco, R., Carulla, M., Condom, M., Alcántara, S., Olivé, M., Planas, A., 1995. Transforming growth factor-alpha immunoreactivity in the developing and adult brain. Neuroscience 66, 189–199.
Fischl, B., Dale, A.M., 2000. Measuring the thickness of the human cerebral cortex from magnetic resonance images. Proc. Natl. Acad. Sci. U. S. A 97, 11050–11055. https://doi.org/10.1073/pnas.200033797.
Fischl, B., Sereno, M.I., Dale, A.M., 1999. Cortical surface-based analysis: II: inflation, flattening, and a surface-based coordinate system. Neuroimage 9, 195–207. https://doi.org/10.1006/nimg.1998.0396.
Frey, S., Campbell, J.S.W., Pike, G.B., Petrides, M., 2008. Dissociating the human language pathways with high angular resolution diffusion fiber tractography. J. Neurosci. 28, 11435–11444. https://doi.org/10.1523/JNEUROSCI.2388-08.2008.
Friederici, A.D., 2012. The cortical language circuit: from auditory perception to sentence comprehension. Trends Cognit. Sci. 16, 262–268. https://doi.org/10.1016/j.tics.2012.04.001.
Friederici, A.D., 2011. The brain basis of language processing: from structure to function. Physiol. Rev. 91, 1357–1392. https://doi.org/10.1152/physrev.00006.2011.
Friederici, A.D., 2009. Pathways to language: fiber tracts in the human brain. Trends Cognit. Sci. https://doi.org/10.1016/j.tics.2009.01.001.
Friederici, A.D., Brauer, J., Lohmann, G., 2011. Maturation of the language network: from inter- to intrahemispheric connectivities. PLoS One 6, 1–7. https://doi.org/10.1371/journal.pone.0020726.
Geng, X., Li, G., Lu, Z., Gao, W., Wang, L., Shen, D., Zhu, H., Gilmore, J.H., 2016. Structural and maturational covariance in early childhood brain development. Cerebr. Cortex. https://doi.org/10.1093/cercor/bhw022 bhw022-.
Ghosh, S.S., Kakunoori, S., Augustinack, J., Nieto-Castanon, A., Kovelman, I., Gaab, N., Christodoulou, J.A., Triantafyllou, C., Gabrieli, J.D.E., Fischl, B., 2010. Evaluating the validity of volume-based and surface-based brain image registration for developmental cognitive neuroscience studies in children 4 to 11years of age. Neuroimage 53, 85–93. https://doi.org/10.1016/j.neuroimage.2010.05.075.
Giedd, J.N., Blumenthal, J., Jeffries, N.O., Castellanos, F.X., Liu, H., Zijdenbos, A., Paus, T., Evans, A.C., Rapoport, J.L., 1999. Brain development during childhood and adolescence: a longitudinal MRI study. Nat. Neurosci. 2, 861–863. https://doi.org/10.1038/13158.
Gong, G., He, Y., Chen, Z.J., Evans, A.C., 2012. Convergence and divergence of thickness correlations with diffusion connections across the human cerebral cortex. Neuroimage 59, 1239–1248. https://doi.org/10.1016/j.neuroimage.2011.08.017.
Gong, G., Rosa-Neto, P., Carbonell, F., Chen, Z.J., He, Y., Evans, A.C., 2009. Age- and gender-related differences in the cortical anatomical network. J. Neurosci. 29, 15684–15693. https://doi.org/10.1523/JNEUROSCI.2308-09.2009.
Greve, D.N., Fischl, B., 2018. False positive rates in surface-based anatomical analysis. Neuroimage 171, 6–14. https://doi.org/10.1016/j.neuroimage.2017.12.072.
Grewe, T., Bornkessel-Schlesewsky, I., Zysset, S., Wiese, R., von Cramon, D.Y., Schlesewsky, M., 2007. The role of the posterior superior temporal sulcus in the processing of unmarked transitivity. Neuroimage 35, 343–352. https://doi.org/10.1016/j.neuroimage.2006.11.045.
Hagmann, P., Sporns, O., Madan, N., Cammoun, L., Pienaar, R., Wedeen, V.J., Meuli, R., Thiran, J.-P., Grant, P.E., 2010. White matter maturation reshapes structural connectivity in the late developing human brain. Proc. Natl. Acad. Sci. Unit. States Am. 107, 19067–19072. https://doi.org/10.1073/pnas.1009073107.
Han, X., Jovicich, J., Salat, D., van der Kouwe, A., Quinn, B., Czanner, S., Busa, E., Pacheco, J., Albert, M., Killiany, R., Maguire, P., Rosas, D., Makris, N., Dale, A., Dickerson, B., Fischl, B., 2006. Reliability of MRI-derived measurements of human cerebral cortical thickness: the effects of field strength, scanner upgrade and manufacturer. Neuroimage 32, 180–194. https://doi.org/10.1016/j.neuroimage.2006.02.051.
Holland, S.K., Plante, E., Weber Byars, A., Strawsburg, R.H., Schmithorst, V.J., Ball, W.S., 2001. Normal fMRI brain activation patterns in children performing a verb generation task. Neuroimage 14, 837–843. https://doi.org/10.1006/nimg.2001.0875.
Honey, C.J., Thivierge, J.P., Sporns, O., 2010. Can structure predict function in the human brain? Neuroimage. https://doi.org/10.1016/j.neuroimage.2010.01.071.
Horn, W., 1983. LPS Leistungsprüfsystem. Hogrefe, Göttingen.
Hosseini, S.M.H., Kesler, S.R., 2013. Comparing connectivity pattern and small-world organization between structural correlation and resting-state networks in healthy adults. Neuroimage. https://doi.org/10.1016/j.neuroimage.2013.04.032.
Hsu, J.-L., Van Hecke, W., Bai, C.-H., Lee, C.-H., Tsai, Y.-F., Chiu, H.-C., Jaw, F.-S., Hsu, C.-Y., Leu, J.-G., Chen, W.-H., Leemans, A., 2010. Microstructural white matter changes in normal aging: a diffusion tensor imaging study with higher-order polynomial regression models. Neuroimage. https://doi.org/10.1016/j.neuroimage.2009.08.031.
Jenkinson, M., Beckmann, C.F., Behrens, T.E.J., Woolrich, M.W., Smith, S.M., 2012. FSL. Neuroimage 62, 782–790. https://doi.org/10.1016/j.neuroimage.2011.09.015.
Kanai, R., Rees, G., 2011. The structural basis of inter-individual differences in human behaviour and cognition. Nat. Rev. Neurosci. 12, 231–242. https://doi.org/10.1038/nrn3000.
Kaufman, A.S., Kaufman, N.L., 1983. Kaufman Assessment Battery for Children. Wiley Online Library.
Kelly, A.M., Di Martino, A., Uddin, L.Q., Shehzad, Z., Gee, D.G., Reiss, P.T., Margulies, D.S., Castellanos, F.X., Milham, M.P., 2009. Development of anterior cingulate functional connectivity from late childhood to early adulthood. Cerebr. Cortex 19, 640–657. https://doi.org/10.1093/cercor/bhn117.
Kinno, R., Kawamura, M., Shioda, S., Sakai, K.L., 2008. Neural correlates of noncanonical syntactic processing revealed by a picture-sentence matching task. Hum. Brain Mapp. 29, 1015–1027. https://doi.org/10.1002/hbm.20441.
Knoll, L.J., Obleser, J., Schipke, C.S., Friederici, A.D., Brauer, J., 2012. Left prefrontal cortex activation during sentence comprehension covaries with grammatical knowledge in children. Neuroimage 62, 207–216. https://doi.org/10.1016/j.neuroimage.2012.05.014.
Krogsrud, S.K., Fjell, A.M., Tamnes, C.K., Grydeland, H., Mork, L., Due-Tønnessen, P., Bjørnerud, A., Sampaio-Baptista, C., Andersson, J., Johansen-Berg, H., Walhovd, K.B., 2016. Changes in white matter microstructure in the developing brain—a longitudinal diffusion tensor imaging study of children from 4 to 11 years of age. Neuroimage 124, 473–486. https://doi.org/10.1016/J.NEUROIMAGE.2015.09.017.
Kumar, R., Nguyen, H.D., Macey, P.M., Woo, M.A., Harper, R.M., 2012. Regional brain axial and radial diffusivity changes during development. J. Neurosci. Res. 90, 346–355. https://doi.org/10.1002/jnr.22757.
Lebel, C., Beaulieu, C., 2011. Longitudinal development of human brain wiring continues from childhood into adulthood. J. Neurosci. 31, 10937–10947. https://doi.org/10.1523/JNEUROSCI.5302-10.2011.
Lebel, C., Gee, M., Camicioli, R., Wieler, M., Martin, W., Beaulieu, C., 2012. Diffusion tensor imaging of white matter tract evolution over the lifespan. Neuroimage. https://doi.org/10.1016/j.neuroimage.2011.11.094.
Lebel, C., Walker, L., Leemans, A., Phillips, L., Beaulieu, C., 2008. Microstructural maturation of the human brain from childhood to adulthood. Neuroimage 40, 1044–1055. https://doi.org/10.1016/j.neuroimage.2007.12.053.
Lee, N.R., Raznahan, A., Wallace, G.L., Alexander-Bloch, A., Clasen, L.S., Lerch, J.P., Giedd, J.N., 2014. Anatomical coupling among distributed cortical regions in youth varies as a function of individual differences in vocabulary abilities. Hum. Brain Mapp. 35, 1885–1895. https://doi.org/10.1002/hbm.22299.
Lerch, J.P., Worsley, K., Shaw, W.P., Greenstein, D.K., Lenroot, R.K., Giedd, J., Evans, A.C., 2006. Mapping anatomical correlations across cerebral cortex (MACACC) using cortical thickness from MRI. Neuroimage 31, 993–1003. https://doi.org/10.1016/j.neuroimage.2006.01.042.
Li, X., Pu, F., Fan, Y., Niu, H., Li, S., Li, D., 2013. Age-related changes in brain structural covariance networks. Front. Hum. Neurosci. 7 https://doi.org/10.3389/fnhum.2013.00098.
Lohmann, G., Hoehl, S., Brauer, J., Danielmeier, C., Bornkessel-Schlesewsky, I., Bahlmann, J., Turner, R., Friederici, A., 2010. Setting the frame: the human brain activates a basic low-frequency network for language processing. Cerebr. Cortex 20, 1286–1292.
Makuuchi, M., Bahlmann, J., Anwander, A., Friederici, A.D., 2009. Segregating the core computational faculty of human language from working memory. Proc. Natl. Acad. Sci. Unit. States Am. 106, 8362–8367. https://doi.org/10.1073/pnas.0810928106.
Mechelli, A., 2005. Structural covariance in the human cortex. J. Neurosci. 25, 8303–8310. https://doi.org/10.1523/JNEUROSCI.0357-05.2005.
Meltzer, J.A., McArdle, J.J., Schafer, R.J., Braun, A.R., 2010. Neural aspects of sentence comprehension: syntactic complexity, reversibility, and reanalysis. Cerebr. Cortex 20, 1853–1864. https://doi.org/10.1093/cercor/bhp249.
Montembeault, M., Joubert, S., Doyon, J., Carrier, J., Gagnon, J.F., Monchi, O., Lungu, O., Belleville, S., Brambati, S.M., 2012. The impact of aging on gray matter structural covariance networks. Neuroimage 63, 754–759. https://doi.org/10.1016/j.neuroimage.2012.06.052.
Montembeault, M., Rouleau, I., Provost, J.S., Brambati, S.M., 2016. Altered gray matter structural covariance networks in early stages of alzheimer's disease. Cerebr. Cortex 26, 2650–2662. https://doi.org/10.1093/cercor/bhv105.
Mukherjee, P., McKinstry, R.C., 2006. Diffusion tensor imaging and tractography of human brain development. Neuroimaging Clin. https://doi.org/10.1016/j.nic.2005.11.004.
Müller-Axt, C., Anwander, A., von Kriegstein, K., 2017. Altered structural connectivity of the left visual thalamus in developmental dyslexia. Curr. Biol. 27, 3692–3698. https://doi.org/10.1016/j.cub.2017.10.034 e4.
Nunez, S.C., Dapretto, M., Katzir, T., Starr, A., Bramen, J., Kan, E., Bookheimer, S., Sowell, E.R., 2011. fMRI of syntactic processing in typically developing children: structural correlates in the inferior frontal gyrus. Dev. Cogn. Neurosci. 1, 313–323. https://doi.org/10.1016/j.dcn.2011.02.004.
Oh, H., Mormino, E.C., Madison, C., Hayenga, A., Smiljic, A., Jagust, W.J., 2011. ??-Amyloid affects frontal and posterior brain networks in normal aging. Neuroimage 54, 1887–1895. https://doi.org/10.1016/j.neuroimage.2010.10.027.
Oldfield, R.C., 1971. The assessment and analysis of handedness: the Edinburgh inventory. Neuropsychologia 9, 97–113. https://doi.org/10.1016/0028-3932(71)90067-4.
Patterson, D.K., Van Petten, C., Beeson, P.M., Rapcsak, S.Z., Plante, E., 2014. Bidirectional iterative parcellation of diffusion weighted imaging data: separating cortical regions connected by the arcuate fasciculus and extreme capsule. Neuroimage 102, 704–716. https://doi.org/10.1016/j.neuroimage.2014.08.032.
Perani, D., Saccuman, M.C., Scifo, P., Anwander, A., Spada, D., Baldoli, C., Poloniato, A., Lohmann, G., Friederici, A.D., 2011. Neural language networks at birth. Proc. Natl. Acad. Sci. Unit. States Am. 108, 16056–16061. https://doi.org/10.1073/pnas.1102991108.
Qi, T., Gu, B., Ding, G., Gong, G., Lu, C., Peng, D., Malins, J.G., Liu, L., 2016. More bilateral, more anterior: alterations of brain organization in the large-scale structural network in Chinese dyslexia. Neuroimage 124, 63–74. https://doi.org/10.1016/j.neuroimage.2015.09.011.
Qiu, D., Tan, L.H., Zhou, K., Khong, P.L., 2008. Diffusion tensor imaging of normal white matter maturation from late childhood to young adulthood: voxel-wise evaluation of

mean diffusivity, fractional anisotropy, radial and axial diffusivities, and correlation with reading development. Neuroimage. https://doi.org/10.1016/j.neuroimage.2008.02.023.

Raznahan, A., Lee, Y., Stidd, R., Long, R., Greenstein, D., Clasen, L., Addington, A., Gogtay, N., Rapoport, J.L., Giedd, J.N., 2010. Longitudinally mapping the influence of sex and androgen signaling on the dynamics of human cortical maturation in adolescence. Proc. Natl. Acad. Sci. Unit. States Am. 107, 16988–16993.

Romero-Garcia, R., Whitaker, K.J., Váša, F., Seidlitz, J., Shinn, M., Fonagy, P., Dolan, R.J., Jones, P.B., Goodyer, I.M., Bullmore, E.T., Vértes, P.E., 2018. Structural covariance networks are coupled to expression of genes enriched in supragranular layers of the human cortex. Neuroimage. https://doi.org/10.1016/j.neuroimage.2017.12.060.

Ruscio, J., Roche, B., 2012. Variance heterogeneity in published psychological research: a review and a new index. Methodology. https://doi.org/10.1027/1614-2241/a000034.

Santi, A., Grodzinsky, Y., 2010. fMRI adaptation dissociates syntactic complexity dimensions. Neuroimage 51, 1285–1293. https://doi.org/10.1016/j.neuroimage.2010.03.034.

Schipke, C.S., Knoll, L.J., Friederici, A.D., Oberecker, R., 2012. Preschool children's interpretation of object-initial sentences: neural correlates of their behavioral performance. Dev. Sci. 15, 762–774. https://doi.org/10.1111/j.1467-7687.2012.01167.x.

Schmithorst, V.J., Wilke, M., Dardzinski, B.J., Holland, S.K., 2002. Correlation of white matter diffusivity and anisotropy with age during childhood and adolescence: a cross-sectional diffusion-tensor MR imaging study. Radiology. https://doi.org/10.1148/radiol.2221010626.

Schmitt, J.E., Lenroot, R.K., Wallace, G.L., Ordaz, S., Taylor, K.N., Kabani, N., Greenstein, D., Lerch, J.P., Kendler, K.S., Neale, M.C., Giedd, J.N., 2008. Identification of genetically mediated cortical networks: a multivariate study of pediatric twins and siblings. Cerebr. Cortex. https://doi.org/10.1093/cercor/bhm211.

Seeley, W.W., Crawford, R.K., Zhou, J., Miller, B.L., Greicius, M.D., 2009. Neurodegenerative diseases target large-scale human brain networks. Neuron 62, 42–52. https://doi.org/10.1016/j.neuron.2009.03.024.

Shaw, P., Kabani, N.J., Lerch, J.P., Eckstrand, K., Lenroot, R., Gogtay, N., Greenstein, D., Clasen, L., Evans, A., Rapoport, J.L., Giedd, J.N., Wise, S.P., 2008. Neurodevelopmental trajectories of the human cerebral cortex. J. Neurosci. 28, 3586–3594. https://doi.org/10.1523/JNEUROSCI.5309-07.2008.

Siegmüller, J., Kauschke, C., von Minnen, S., Bittner, D., 2011. TSVK Test zum Satzverstehen von Kindern.

Silbereis, J.C., Pochareddy, S., Zhu, Y., Li, M., Sestan, N., 2016. The cellular and molecular landscapes of the developing human central nervous system. Neuron. https://doi.org/10.1016/j.neuron.2015.12.008.

Skeide, M.A., Brauer, J., Friederici, A.D., 2016. Brain functional and structural predictors of language performance. Cerebr. Cortex 26, 2127–2139. https://doi.org/10.1093/cercor/bhv042.

Skeide, M.A., Brauer, J., Friederici, A.D., 2014. Syntax gradually segregates from semantics in the developing brain. Neuroimage 100, 106–111. https://doi.org/10.1016/j.neuroimage.2014.05.080.

Skeide, M.A., Friederici, A.D., 2016. The ontogeny of the cortical language network. Nat. Rev. Neurosci. https://doi.org/10.1038/nrn.2016.23.

Smith, S.M., Jenkinson, M., Woolrich, M.W., Beckmann, C.F., Behrens, T.E.J., Johansen-Berg, H., Bannister, P.R., De Luca, M., Drobnjak, I., Flitney, D.E., Niazy, R.K., Saunders, J., Vickers, J., Zhang, Y., De Stefano, N., Brady, J.M., Matthews, P.M., 2004. Advances in functional and structural MR image analysis and implementation as FSL. Neuroimage. https://doi.org/10.1016/j.neuroimage.2004.07.051.

Song, S.K., Sun, S.W., Ramsbottom, M.J., Chang, C., Russell, J., Cross, A.H., 2002. Dysmyelination revealed through MRI as increased radial (but unchanged axial) diffusion of water. Neuroimage. https://doi.org/10.1006/nimg.2002.1267.

Song, S.K., Yoshino, J., Le, T.Q., Lin, S.J., Sun, S.W., Cross, A.H., Armstrong, R.C., 2005. Demyelination increases radial diffusivity in corpus callosum of mouse brain. Neuroimage. https://doi.org/10.1016/j.neuroimage.2005.01.028.

Sowell, E.R., 2004. Longitudinal mapping of cortical thickness and brain growth in normal children. J. Neurosci. 24, 8223–8231. https://doi.org/10.1523/JNEUROSCI.1798-04.2004.

Sowell, E.R., Thompson, P.M., Toga, A.W., 2004. Mapping changes in the human cortex throughout the span of life. Neuroscientist. https://doi.org/10.1177/1073858404263960.

Stevens, M.C., Pearlson, G.D., Calhoun, V.D., 2009. Changes in the interaction of resting-state neural networks from adolescence to adulthood. Hum. Brain Mapp. https://doi.org/10.1002/hbm.20673.

Supekar, K., Musen, M., Menon, V., 2009. Development of large-scale functional brain networks in children. PLoS Biol. 7 https://doi.org/10.1371/journal.pbio.1000157.

Suzuki, Y., Matsuzawa, H., Kwee, I.L., Nakada, T., 2003. Absolute eigenvalue diffusion tensor analysis for human brain maturation. NMR Biomed. https://doi.org/10.1002/nbm.848.

Tamnes, C.K., Østby, Y., Fjell, A.M., Westlye, L.T., Due-Tønnessen, P., Walhovd, K.B., 2010. Brain maturation in adolescence and young adulthood: regional age-related changes in cortical thickness and white matter volume and microstructure. Cerebr. Cortex. https://doi.org/10.1093/cercor/bhp118.

Tomasi, D., Volkow, N.D., 2012. Resting functional connectivity of language networks: characterization and reproducibility. Mol. Psychiatr. 17, 841–854. https://doi.org/10.1038/mp.2011.177.

Valk, S.L., Bernhardt, B.C., Böckler, A., Trautwein, F.-M., Kanske, P., Singer, T., 2016. Socio-cognitive phenotypes differentially modulate large-scale structural covariance networks. Cerebrum. Cortex. https://doi.org/10.1093/cercor/bhv319 bhv319.

Valk, S.L., Bernhardt, B.C., Trautwein, F.M., Böckler, A., Kanske, P., Guizard, N., Louis Collins, D., Singer, T., 2017. Structural plasticity of the social brain: differential change after socio-affective and cognitive mental training. Sci. Adv. 3 https://doi.org/10.1126/sciadv.1700489.

Vissiennon, K., Friederici, A.D., Brauer, J., Wu, C.-Y., 2017. Functional organization of the language network in three-and six-year-old children. Neuropsychologia 98, 24–33.

Westlye, L.T., Walhovd, K.B., Dale, A.M., Bjørnerud, A., Due-Tønnessen, P., Engvig, A., Grydeland, H., Tamnes, C.K., Østby, Y., Fjell, A.M., 2010. Life-span changes of the human brain white matter: diffusion tensor imaging (DTI) and volumetry. Cerebr. Cortex. https://doi.org/10.1093/cercor/bhp280.

Whitaker, K.J., Vértes, P.E., Romero-Garcia, R., Váša, F., Moutoussis, M., Prabhu, G., Weiskopf, N., Callaghan, M.F., Wagstyl, K., Rittman, T., Tait, R., Ooi, C., Suckling, J., Inkster, B., Fonagy, P., Dolan, R.J., Jones, P.B., Goodyer, I.M., Bullmore, E.T., 2016. Adolescence is associated with genomically patterned consolidation of the hubs of the human brain connectome. Proc. Natl. Acad. Sci. Unit. States Am. https://doi.org/10.1073/pnas.1601745113.

Wilson, S.M., Galantucci, S., Tartaglia, M.C., Rising, K., Patterson, D.K., Henry, M.L., Ogar, J.M., DeLeon, J., Miller, B.L., Gorno-Tempini, M.L., 2011. Syntactic processing depends on dorsal language tracts. Neuron 72, 397–403. https://doi.org/10.1016/j.neuron.2011.09.014.

Woolrich, M.W., Jbabdi, S., Patenaude, B., Chappell, M., Makni, S., Behrens, T., Beckmann, C., Jenkinson, M., Smith, S.M., 2009. Bayesian analysis of neuroimaging data in FSL. Neuroimage 45. https://doi.org/10.1016/j.neuroimage.2008.10.055.

Worsley, K.J., Andermann, M., Koulis, T., MacDonald, D., Evans, A.C., 1999. Detecting changes in nonisotropic images. Hum. Brain Mapp. 98–101. https://doi.org/10.1002/(SICI)1097-0193(1999)8:2/3<98::AID-HBM5>3.0.CO;2-F.

Wu, C.Y., Vissiennon, K., Friederici, A.D., Brauer, J., 2016. Preschoolers' brains rely on semantic cues prior to the mastery of syntax during sentence comprehension. Neuroimage 126, 256–266. https://doi.org/10.1016/j.neuroimage.2015.10.036.

Xiao, Y., Friederici, A.D., Margulies, D.S., Brauer, J., 2016. Development of a selective left-hemispheric fronto-temporal network for processing syntactic complexity in language comprehension. Neuropsychologia 83, 274–282. https://doi.org/10.1016/j.neuropsychologia.2015.09.003.

Yap, Q.J., Teh, I., Fusar-Poli, P., Sum, M.Y., Kuswanto, C., Sim, K., 2013. Tracking cerebral white matter changes across the lifespan: insights from diffusion tensor imaging studies. J. Neural. Transm. https://doi.org/10.1007/s00702-013-0971-7.

Yeatman, J.D., Wandell, B.A., Mezer, A.A., 2014. Lifespan maturation and degeneration of human brain white matter. Nat. Commun. https://doi.org/10.1038/ncomms5932.

Yee, Y., Fernandes, D.J., French, L., Ellegood, J., Cahill, L.S., Vousden, D.A., Spencer Noakes, L., Scholz, J., van Eede, M.C., Nieman, B.J., Sled, J.G., Lerch, J.P., 2018. Structural covariance of brain region volumes is associated with both structural connectivity and transcriptomic similarity. Neuroimage. https://doi.org/10.1016/j.neuroimage.2018.05.028.

Zhang, J., Evans, A., Hermoye, L., Lee, S.K., Wakana, S., Zhang, W., Donohue, P., Miller, M.I., Huang, H., Wang, X., van Zijl, P.C.M., Mori, S., 2007. Evidence of slow maturation of the superior longitudinal fasciculus in early childhood by diffusion tensor imaging. Neuroimage 38, 239–247. https://doi.org/10.1016/j.neuroimage.2007.07.033.

Zielinski, B.A., Gennatas, E.D., Zhou, J., Seeley, W.W., 2010. Network-level structural covariance in the developing brain. Proc. Natl. Acad. Sci. Unit. States Am. 107, 18191–18196. https://doi.org/10.1073/pnas.1003109107.